

Effect of compatibilizer and nanosilica on the mechanical, thermal, and degradation kinetic properties of polypropylene/polylactic acid blends

Aravind Raj, Pachipala Rithik, Prathipati Sai Sudheer, Kedarisetty Sampath Vachan,
Murugasamy Kannan*

Department of Chemical Engineering and Materials Science, Amrita School of Engineering, Coimbatore-641112,
Amrita Vishwa Vidyapeetham, India

Received: 21 July 2023, Accepted: 23 November 2023

ABSTRACT

In this study, polypropylene (PP) was blended with polylactic acid (PLA) to enhance PP's mechanical properties, such as tensile strength and modulus, and to encourage the adoption of eco-friendly, renewable resource based material in polymer production. Even though PLA's biodegradability cannot be fully utilized in PP/PLA blends, but PLA can still improve PP's mechanical properties and provide an alternative resource for biobased raw materials. To meet the requirement, PP and PLA were blended in a 70:30 ratios with a compatibilizer and nanosilica at different loading levels by melt-blending. Blends of PP and PLA materials were processed without any problems, since both materials have melting points in the range of 170°C. Despite this, the properties of polymer blends are limited by the immiscibility between these neat polymers. To solve this problem, compatibilizers like polypropylene-grafted-maleic anhydride (PP-g-MA) were added to blends to improve their compatibility. Nanosilica was also added to this compatibilizer to study the system's compatibility and modify the hydrophobicity of PLA. Differential scanning calorimetry (DSC), thermogravimetric analysis (TGA), Fourier transform infrared spectroscopy (FTIR), tensile strength, and field emission scanning electron microscopy (FESEM) were used to analyze the polymer blend. Results indicate that compatibilizers play a significant role in improving tensile properties, thermal stability, and blend dispersion in the system, mainly in 5 parts compatibilizer-based systems. Composition with 5 parts compatibilizer increases tensile strength of 70/30 blend from 19.7 to 27 MPa, while elongation increases from 2.2 to 3.6 %. Additionally, a composition with 0.7 parts of nanosilica increases the modulus from 1488 to 1732 MPa when compared to the 70/30 blend. **Polyolefins J (2024) 11: 43-59**

Keywords: PP based blends; processability; thermal degradation; thermal properties; SEM images.

INTRODUCTION

We live in a world of polymers and all major field industries depend on them, from automobiles to space, as well as textile and food packaging. Among all polymers, Polypropylene, commonly known as PP, is a thermoplastic material featuring moderate mechanical properties, reasonable barrier properties, flexibility, thermal stability, low cost, light weight, and chemical inertness. It ranks among the world's most widely consumed polymers, finding applications in diverse sectors like packaging, house hold goods, automotive,

textiles, and medical field [1]. To further enhance the performance properties and expand the application ranges, various polyblend nanocomposites based on PP were prepared and characterized. However, PP is not a biodegradable material and is manufactured from nonrenewable petroleum based resources. The consequences of this led to global concerns about the environment. Crude oil is now used to make monomers that make plastics. It is possible that continued use of crude oil for plastic may not be sustainable and could

*Corresponding Author - E-mail: m_kannan@cb.amrita.edu

result in even greater pollution [2-4].

One of the approaches to solving these problems could involve replacing or reducing the use of non-biodegradable and petroleum-based plastics with biodegradable plastics made from renewable resources. In the bioplastic world, polylactic acid (PLA) is one of the most common types. PLA is made up of lactic acid monomers, which are manufactured from renewable sources like corn. Due to its eco-friendliness, biocompatibility, renewable nature, high tensile strength and modulus, and biodegradability, PLA is one of the important polymers [5,6]. On the other hand, due to PLA's brittleness, poor thermal stability and melt strength for processing, and its poor water resistance and oxygen barrier properties, it is not suitable for a wide range of other applications [7-9]. Hence, blending PP with PLA could yield a novel material with the desired performance, such as an increase in tensile strength and modulus compared to PP, all at a reasonable cost. Despite this, PP and PLA are partially immiscible and lead for multiphase blends with low mechanical and barrier properties. This miscibility can be improved by adding compatibilizing agents and nanofillers. The following available research reports in this field have been reviewed, and based on these studies, a suitable compatibilizer and nanofiller have been selected to evaluate the PP/PLA blends for better performance.

Guopeng and coworkers [10] compared the effects of adding ethylene-(methyl acrylate)-(glycidyl methacrylate) (EMA-GMA) as a reactive compatibilizer for PP/PLA blends. They found that adding the compatibilizer under relatively low shear force was more efficient than under high shear force without the compatibilizer. Xu et al. [11] performed a study in which an ethylene-glycidyl methacrylate-methyl acrylate terpolymer (PEGMMA) was utilized as a reactive compatibilizer for PLA blended with polypropylene (PP). The blends exhibited substantial improvements in elongation at break and tensile toughness compared to the corresponding binary blends. Choudhary et al. [12] conducted studies on the presence of PP grafted maleic anhydride (PP-g-MA) compatibilizer in PLA/PP blends with PLA in ratios of 90/10, 80/20, 70/30, and 50/50 to PP. The results indicated an increase in tensile strength, modulus, and impact strength for 90/10 composition.

Rajan and coworkers [13] prepared a PP-rich blend with PLA and found that, based on rheological measurements and mechanical properties, 3 wt.% of the PP-g-MA compatibilizer effectively enhanced

the compatibility of the selected blend composition. Yoo et al. [14] formulated polyblends of PP and PLA in an 80:20 ratio, employing PP-g-MA and styrene-ethylene-butylene-styrene-g-maleic anhydride (SEBS-g-MA) as compatibilizers. For the PP/PLA (80/20) blends before and after hydrolysis, the impact strength of the blends increased with the SEBS-g-MA content. Ebadi-Dehaghani et al. [15] examined the dynamic rheological behavior of PP-rich (75/25) and PLA-rich (25/75) systems with a terpolymer of ethylene, butyl acrylate, and glycidyl methacrylate as a compatibilizer. Morphological studies revealed a 100% reduction in the size of PLA domains in the compatibilized PP-rich system containing 5 wt.% of the compatibilizer. Such rigorous domain size reduction was not observed for the PLA-rich system.

Li et al. [16] investigated the impact of maleic anhydride and PP-g-MA as individual compatibilizers as well as their combined effect on an 80:20 blend of PLA and PP. Their compatibility was enhanced by MA and PP-g-MA, with PP-g-MA showing a stronger effect than MA. This is because MA has a stable ring structure and a lower grafting proportion in the PLA/MA/PP composition. The compatibilized polyblend nanocomposites of PP/PLA at an 80:20 ratio with varying amounts of halloysite nanotubes (HNT) were reported in the work of Rajan et al. [1]. In this study, an increase in viscosity was observed after adding HNT in the rheology analysis with a compatibilizer, indicating an improvement in the interaction between the nanofiller and the matrix.

Bhasney et al. [17] studied a PLA/PP blend in an 80/20 ratio with the addition of microcrystalline cellulose (MCC) as a nanofiller. It was observed that there was a marginal enhancement in tensile strength and a decline in % elongation due to the reinforcement and orientation of the MCC fibers in the PLA80/19.9PP/0.1MCC biocomposites. Bai and colleagues [18] conducted research on PLA/PP blends, examining compositions with a high PLA content and high PP content while employing PP-g-MA as a compatibilizer. It shows that the thermal stability of the blend was improved by PP, and the incorporation of PP-g-MA further enhanced the thermal stability, although it led to a reduction in the tensile strength of the blend. In PP rich compositions, adding a compatibilizer increases the tensile strength, whereas this effect was not observed in PLA-rich compositions.

There are several benefits to using renewable resource-based PLA in a PP/PLA blend. These include reducing the use of petroleum-based plastics,

improving the biodegradability of the blend, and supporting the development of a more sustainable plastics industry [19]. In this study, PLA is chosen as the material to melt blend with PP in a ratio of 70 parts PP to 30 parts PLA. The selection of the 70/30 ratio for the PP/PLA blend in this study is based on these considerations. Blending PP and PLA in a 70/30 ratio combines the average mechanical properties, low cost, good processability, moisture resistance and heat resistance of PP with the biodegradability and environmental advantages of PLA, providing an alternative resource for bio-based raw materials. Furthermore, in the existing literature survey for this blend-based study, the commonly used ratio is 70/30. The blend of PP and PLA materials are processed without any problem because both materials' melting points are in the range of 170°C. These neat polymers are not miscible, which limits the properties of polymer blends. To overcome this problem, compatibilizers like polypropylene-grafted-maleic anhydride (PP-g-MA), are used to improve the compatibility of immiscible blends. With these compatibilizer another nanofiller nanosilica is added to study the compatibility of the system and to modify the hydrophobicity of the PLA.

This present work differs significantly due to the selection of a hydrophilic nanosilica and PP-g-MA compatibilizer combination. The novelty of this method lies in its potential to create a synergistic effect within this combination, as well as in the role of hydrophilic nanosilica in modifying interfacial adhesion and its effect on the hydrolysis of PLA ester groups.

EXPERIMENTAL

Materials

Polylactic acid grade of Ingeo 4043D was purchased

from NatureWorks© LLC, Minnetonka, MN, USA with a density of 1.24 g/cm³, number average molecular weight of (5.5 x 10⁴) 55,000 g/mol and polydispersity index of 1.62. PP with melt flow index of 11 g/10 minute (230°C /2.16 kg) was purchased from Reliance Industries Ltd, India; the grade of PP is Repol H110MA (PDI value:4.25). PP-g-MA was procured from DuPont (Grade: Fusabond P M613-05). The maleic anhydride content level in PP-g-MA is 1%, and its MFI value is 49 (measured at 190°C with a load of 1.0 kg). Nanosilica was supplied by Sigma Aldrich (Particle size: 50-60 nm).

Sample preparation

The melt method was used to blend polymers for this work because it is the most convenient and suitable for enhancing their properties or modifying their properties. PP-g-MA and nanosilica were added in 1, 5 and 7 parts to improve the properties of the blend. Initially, the basis of the blend was taken as 100 g with a 70% proportion of PP and 30% proportion of PLA. PP-g-MA and nanosilica were added in extra parts. PP, PLA, PP-g-MA and nanosilica were blended in a corotating twin screw extruder (TSE) with the sample composition shown in the Table 1. The twin screw extruder used was manufactured by Aasabi Machinery Ltd, India.

The ratio of PP-g-MA and nanosilica in the blend was varied to improve its properties. The TSE consists of three zones: one feed zone, one compression zone and one metering zone, and the temperature was maintained in the range of 170 to 210°C and the screw was operated at 25 rpm. The materials PP, PLA, PP-g-MA and nanosilica are fed into the feed zone according to their ratios. In the metering zone, the material melts completely after passing through the compression zone, producing melt strands. The

Table 1. Sample compositions (Parts in g).

Sample No.	Polypropylene(PP) parts	Polylactic acid (PLA) parts	Compatibilizer (PP-g-MA) parts	Nano filler-Nano silica parts
1	70	30	-	-
2	70	30	2	-
3	70	30	5	-
4	70	30	7	-
5	70	30	-	0.2
6	70	30	2	0.2
7	70	30	-	0.5
8	70	30	5	0.5
9	70	30	-	0.7
10	70	30	7	0.7
11	100	-	-	-
12	-	100	-	-

molten strand was cooled in cooling baths and left to dry in the atmosphere. The dried strand was converted to pellets by using a granulator machine.

The intermediate product pellet was dried in an oven at 105°C for 2h and fed into the injection molding hopper. It was melted uniformly and injected into the mold and finally the solidified testing sample was removed from the mold. The sigma model injection molding machine was used, manufactured by Ferromatik Milacron, India. The injection molding unit has three zones covering a temperature range of 170 to 190°C and a nozzle maintained at 180°C. After cooling the final product was obtained in a dumbbell shape with dimensions of 125 mm in length, 3.5 mm in thickness and 14 mm in width. The impact of nanosilica and PP-g-MA was analyzed based on the results of mechanical and thermal tests.

Testing and characterization

Tensile test

In this analysis the sample was subjected to loads in incremental mode and the corresponding elongation was measured and plotted as stress-strain curve. Five samples of each composition were tested, and their average values are reported. Properties such as tensile strength, modulus, and elongation were calculated using these tensile test results. The equipment used for this test is Tinius Olsen, UK make H25KT universal testing machine (UTM). The rate of jaw movement was fixed at 50 mm/min. As per ASTM D638 standard, tensile tests were conducted.

Thermogravimetric analysis (TGA)

During the heating of a sample at a constant rate, a TGA analyzer monitors the weight change in proportion to the change in temperature or time. This results in the determination of the material's thermal stability and its composition fractions. The TGA enables the study of physical phenomena such as mass loss or absorption and chemical phenomena such as chemisorption, thermal decomposition, etc. A kinetic study of thermal degradation can be performed from the TGA results by using Coats-Redfern Equation. In this study, the sample was heated at a rate of 10°C per minute. The result from TGA gives the initial and final weight of the sample and weight percentage present at temperature. The DTG (derivative thermogravimetric) curve peak gives the differential peak degradation temperature which is used in kinetic study. The kinetic study of degradation aims to determine the degradation rate, activation energy,

enthalpy, and Gibbs free energy of the sample during the degradation process. The analysis explains which composition is getting degraded at lower and higher temperatures, which indicates the sample's thermal stability. The equipment used for this TGA analysis is thermogravimetric analyzer of model SDTQ600, manufactured by TA Instruments, Delaware, U.S.A. Coats- Redfern Equation [20]:

$$\ln \left[\frac{g(\alpha)}{T^2} \right] = \ln \left\{ \frac{AR}{\phi E_a} \right\} - \frac{E_a}{RT} \quad (1)$$

Where, E_a = activation energy, A = pre-exponential factor, R = universal gas constant, T = Temperature, ϕ is the heating rate.

Activation Energy can be found from the slope by plotting $\ln \frac{g(\alpha)}{T^2}$ vs $\frac{1}{T}$, whereas the pre-exponential factor is found from the intercept. $g(\alpha)$ has different expressions in terms of conversion, the expression for $g(\alpha)$ chosen for this study is $\ln(1-\alpha)$ Where α is the conversion of degradation of the sample.

$$\alpha = \frac{w_i - w_t}{w_i - w_f} \quad (2)$$

where w_i = the initial weight of the sample; w_t = the weight of the sample present at that particular temperature (T); w_f = the final weight of the sample. The change of enthalpy is calculated using the activation energy by the formula:

$$\Delta H = E - RT_p \quad (3)$$

where E = activation energy, R = universal gas constant and T_p = differential peak degradation temperature which is found from DTG curve.

The change of entropy is also calculated using the formula:

$$\Delta S = 2.303 \log \left(\frac{Ah}{k_B T_p} \right) \quad (4)$$

where A = pre-exponential factor, h = Planck's constant and k_B = Boltzmann's constant.

The change in Gibbs free energy was also calculated using the formula:

$$\Delta G = \Delta H - T_p \Delta S \quad (5)$$

Negative values of ΔH indicate an exothermic

degradation reaction, and positive values indicate an endothermic degradation reaction. The positive value of ΔG indicates that the reaction is nonspontaneous and negative value indicates it is spontaneous reaction.

Differential Scanning Calorimetry (DSC)

As a function of time and temperature, differential scanning calorimetry (DSC) measures temperatures and heat flows associated with transitions in materials. The properties obtained from DSC are glass transition temperature (T_g), melting temperature (T_m), heat of fusion (H_f), and crystallization temperature (T_c). DSC consists of a reference sample and the given sample maintained in certain atmospheric conditions, the amplifier maintains zero temperature difference between the reference sample and the given sample. The energy exchanged from or to the given sample to maintain the same temperature with reference sample is measured and observed. The equipment used for DSC analysis is the DSC Q20 V24.11, TA Instruments, Delaware, U.S.A. The test was conducted in a Nitrogen atmosphere with a heating rate of $10^\circ\text{C}/\text{min}$. The heating was conducted for a temperature range of room temperature to 400°C .

The degree of crystallinity (χ_c) of the PLA-based composites was determined using the following equation [5]:

$$\chi_c = 100\% \times \left(\frac{\Delta H_m - \Delta H_{cc}}{\Delta H_m^o} \right) \times \frac{1}{W_{PLA}} \quad (6)$$

Here, ΔH_m represents the melting enthalpy of the sample (Jg^{-1}); ΔH_m^o stands for the melting enthalpy of 100% crystalline PLA (93.0 Jg^{-1}); W_{PLA} denotes the weight fraction of PLA in the composite, and ΔH_{cc} signifies the cold crystallization enthalpy.

Fourier Transform Infrared Spectroscopy (FTIR)

When infrared radiation is passed through a sample, some of the energy is absorbed by the sample and the rest is transmitted. The resulting spectrum represents the absorption and transmission of molecules in the sample. In this study, a sample was analyzed by FTIR in ATR (attenuated total reflection) mode. The Fourier transform infrared spectrometer of model Alpha II, Bruker, Billerica, Massachusetts, U.S.A was used for FTIR analysis.

Field Emission Scanning Electron Microscopy (FE-SEM)

Analyzing the PP/PLA blend and nanoparticle dispersion within the given composition is particularly

useful for correlating other properties. SEM analysis was conducted after failure of the tensile specimen, which is used for the test. At that failure cross section, the specimen was coated with gold particles to make the surface conductive. As seen in the image, PLA content was visible as holes; the holes indicate that PLA was pulled out at the time of tensile test failure. FE-SEM analysis was performed using Zeiss Gemini SEM 300, Carl Zeiss, Germany.

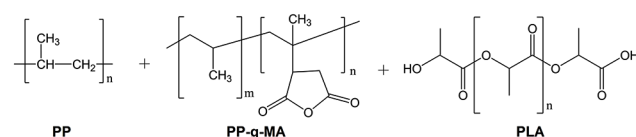
RESULTS AND DISCUSSION

Tensile test

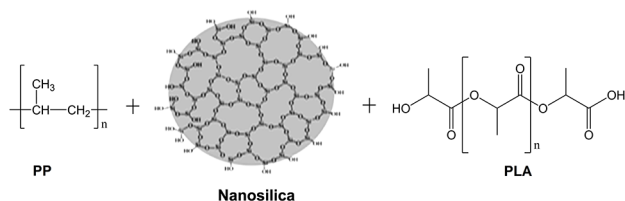
The reported tensile strength values for neat PP, neat PLA, and PP/PLA (70/30) were recorded as 24.1, 46.1, and 19.7 MPa, respectively, as shown in Figure 1(a). This study indicates that the tensile strength of the PP material decreased from 24.1 to 19.7 MPa after blending with PP/PLA in a 70/30 ratio. However, the addition of a compatibilizer to this blend increased the tensile strength to as high as 27 MPa for a 5-part compatibilizer (Figures 1(a) and 1(b)), and this value is higher than that of neat PP. It was also observed that the PP/PLA blend with a compatibilizer included in its composition demonstrates higher tensile strength than neat PP, as shown in Figures 1(a) and 1(b).

When 3, 5 and 7 parts of compatibilizer were added, the tensile strength was reported to be 25.2, 27.0, and 25.7 MPa, respectively. Enhanced tensile strength may be due to better interaction between maleic anhydride moiety and PLA chain end - OH group (Scheme 1). The tensile strength improves with an increase in compatibilizer, but after 5 parts, the results drop. It indicates the by adding more quantity of PP-g-MA to this compound, tensile strength may be reduced for 7 parts of compatibilizer. When grafting MA with PP, PP molecular weight was reduced due to benzoyl peroxide based free radical mechanism involving chain scission. MA content in this compatibilizer is only 1%, but main content is PP.

For nanosilica incorporation, reported tensile strength values were 19.5, 24.5, and 16.1 MPa for



Scheme 1. Chemical structure of PP, PLA and PP-g-MA compatibilizer.



Scheme 2. Chemical structure of PP, PLA and nanosilica.

0.2, 0.5, and 0.7 parts, respectively (Figure 1(b)). Nanosilica's more hydrophilic nature may have resulted in less interaction in this blend, contributing to the less significant improvement of tensile strength (Scheme 2) [21,22]. Adding compatibilizer and nanosilica showed improvement in tensile strength, and this may be compatibilizer's presence (Figure 1 (b)). The highest recorded tensile strength of the blends was 27.0 MPa with 5 parts of compatibilizer alone. In this study indicates that the elongation of the neat blend was increased from 2.2% to higher side for all other composition [23,24]. An elongation of 3.6 % was found in the composition with 5 parts, which indicates a comparatively better interaction between PLA and PP (Figure 1(c)).

In a polymer blend or composite system, the interface refers to the boundary between two distinct phases or materials. These materials often have different chemical or physical properties, leading to poor adhesion between them. This can result in weak interfaces, poor mechanical properties, and reduced overall performance of the composite material. When an external load is applied to the composite, stress is transferred from one phase to the other at the interface. If the interface is weak and poorly bonded, stress concentrations can occur, leading to premature failure of the material. A well-chosen compatibilizer enhances the stress transfer across the interface. Interface modification involves altering the characteristics of this boundary region to improve compatibility between the phases [25,26].

The use of the PP-g-MA compatibilizer tackles the challenges arising from the immiscibility of PP and PLA within blends. Through the establishment of improved interfacial adhesion, the compatibilizer enhances stress transfer across the interface, resulting in improved mechanical properties and overall performance. The PP-g-MA compatibilizer is a

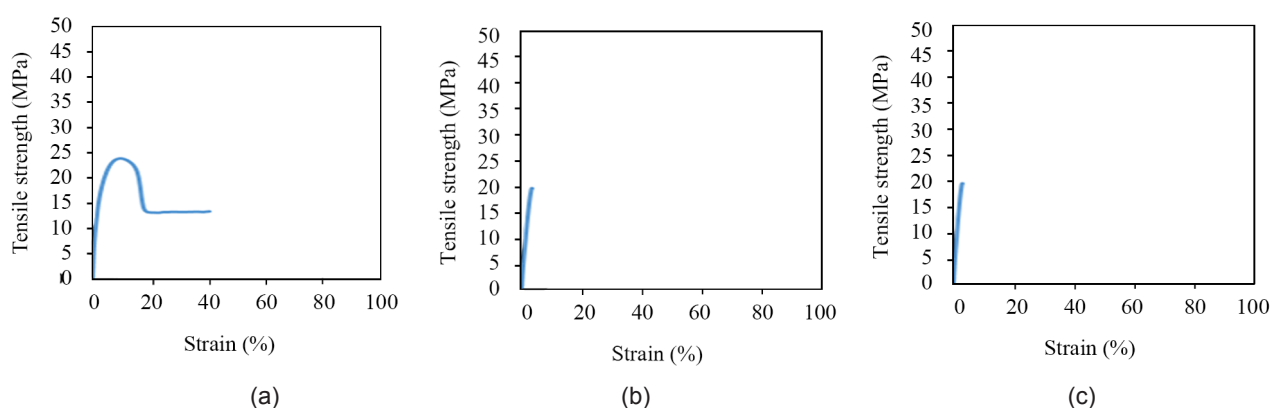


Figure 1(a). Tensile test: Stress –strain curve of neat PP, neat PLA, and PP/PLA (70/30).

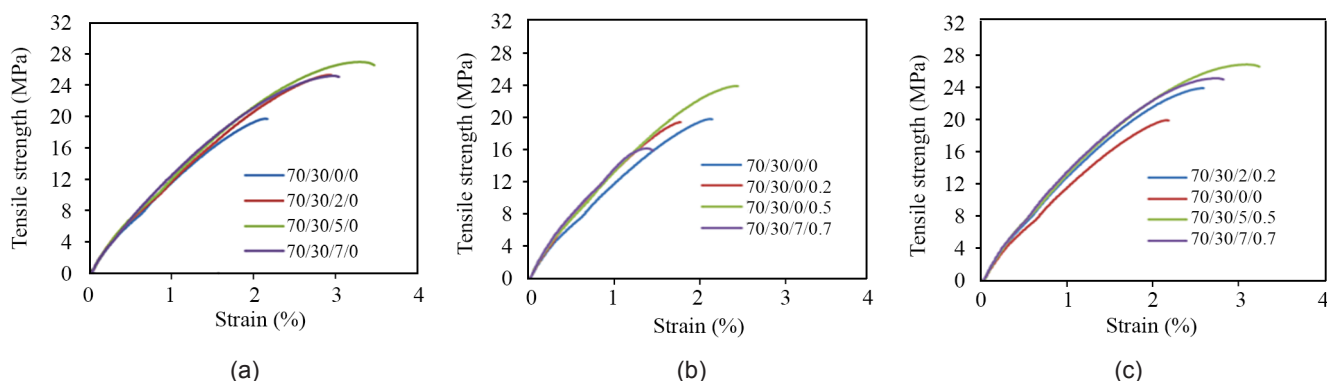


Figure 1(b). Tensile test: (a) containing compatibilizer only (b) containing nanosilica only (c) combination of nanosilica and compatibilizer.

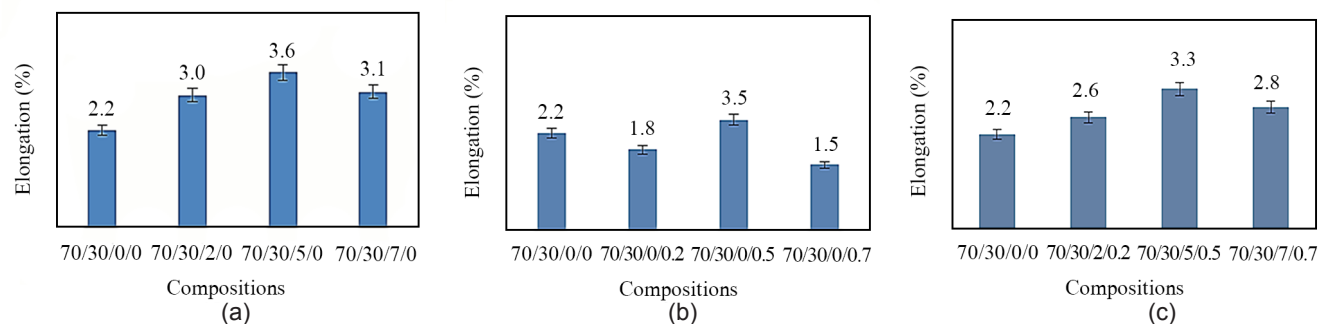


Figure 1(c) Tensile test: elongation analysis (a) compatibilizer (b) nanosilica (c) nanosilica and compatibilizer.

compound that contains both polypropylene segments and maleic anhydride functional groups. These functional groups are key to its role in improving the compatibility of PP and PLA, which are inherently incompatible due to their differing chemical structures and polarities. The PP portion of the compatibilizer becomes compatible with PP in the blend, while the maleic anhydride groups have an affinity for polar groups such as the $-OH$ end group and ester group present in PLA. This affinity allows for improved adhesion between the two polymers.

In the case of a nanosilica based composition, the hydrophilic nature of nanosilica may have led to a potential interaction with the PLA component in this blend, rather than with the PP component. As a result, a significant improvement in tensile strength was not observed, but due to nanosilica's reinforcement effect, all nanosilica-based compositions have a higher modulus.

However, in a compatibilizer and nanosilica based composition, there is a possibility for the formation of hydrogen bonding between nanosilica and the compatibilizer. This interaction may not directly alter the matrix properties.

Table 2. Mechanical properties.

Composition (PP/PLA/PP-g-MA)/Nanosilica)	Tensile strength (MPa)	Elongation %	Modulus MPa
100/0/0/0	24.1	40.5	1330
0/100/0/0	46.1	2.5	2370
70/30/0/0	19.7	2.2	1488
70/30/2/0	25.2	3.0	1538
70/30/5/0	27.0	3.6	1561
70/30/7/0	25.7	3.1	1527
70/30/0/0.2	19.5	1.8	1528
70/30/0/0.5	24.5	2.5	1674
70/30/0/0.7	16.1	1.6	1732
70/30/2/0.2	23.8	2.6	1585
70/30/5/0.5	27.0	3.3	1622
70/30/7/0.7	24.5	2.8	1707

Even though, after the interaction between nanosilica and the compatibilizer, the nonpolar PP portion of the PP-g-MA is compatible with the nonpolar PP in the blend, the polar nature of the hydrophilic nanosilica is expected to interact with the $-OH$ end group and ester group of PLA. This interaction may be the reason for the improvement in the tensile strength of this composition.

Based on Figure 1, these stress-strain curves show that the modulus of all compositions based on compatibilizer and nanosilica is higher than that of the neat PP. Modulus values for all compositions were calculated and are shown in Table 2. This is due to the fact that PLA has a high modulus compared to PP, and there is a possibility of reducing the interfacial tension between PP and PLA after adding a compatibilizer in the system. Additionally, nanosilica plays a role as a reinforcement material in the system.

Overall, the addition of a compatibilizer alone or in combination with nanosilica to this PP/PLA blend improves its tensile strength and modulus. This alignment with the goal of creating more sustainable materials is achieved by blending PLA with PP.

Thermogravimetric Analysis

In this study, the TGA curves displayed a two-step degradation process for all PP/PLA blends, except for neat PP and neat PLA. This indicates that the degradation of PLA material in the blend occurs first, followed by PP degradation. The presence of ester bonds in PLA makes it more susceptible to hydrolysis and degradation. On the other hand, PP is a synthetic polymer with a stable hydrocarbon backbone. This property renders PP more resistant to hydrolysis and thermal degradation, necessitating higher temperatures to break down its molecular structure.

The thermogravimetric analysis (TGA) curves are shown in Figures 2, 3, and 4, respectively. Figures 2, 3 and 4 are the merged graphs of compatibilizers

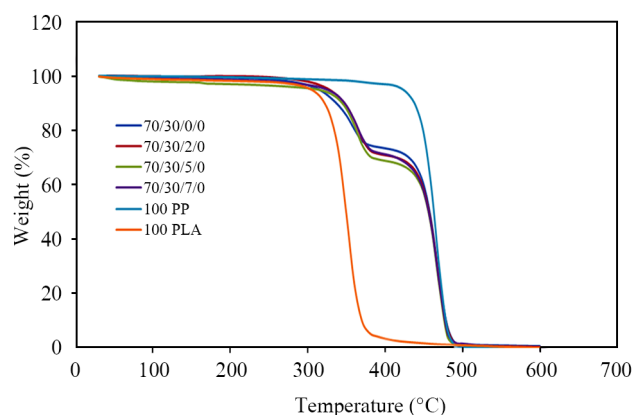


Figure 2. TGA curve of neat PLA, neat PP and PP/PLA blend with compatibilizer at different parts.

with various parts, nanosilica with various parts, and compatibilizers and nano silica with various parts, respectively. Figure 2 represents the TGA curves of the compatibilizers with PP-g-MA 2, 5, and 7 parts. Figure 3 represents the TGA curves of polymer blends with nanosilica loaded in the absence of compatibilizer. The nanosilica was loaded in the blend with 0.2, 0.5, and 0.7 parts, respectively. Figure 4 represents the TGA curves of both compatibilizer PP-g-MA and nano filler nanosilica added to the PP/PLA blend in PP-g-MA 2 parts, nanosilica 0.2 parts; PP-g-MA 5 parts, nano silica 0.5 parts and PP-g-MA 7 parts, nanosilica 0.7 parts. As mentioned earlier, all TGA curves show a two-step degradation, except for the neat materials.

A comparison of the thermal degradation of PP/PLA neat blend with PP-g-MA compatibilizer added to this neat blend was shown in Figure 2. Initial weight losses were observed from about 300 to 370°C for PLA in the blend. Figure 2 shows that all the graphs for the blends were bound between neat PLA and neat PP;

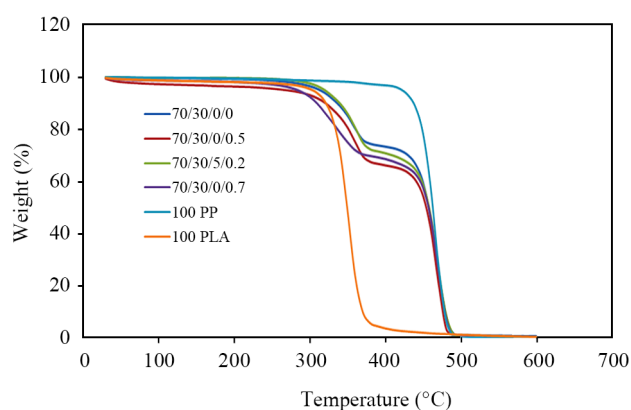


Figure 3. TGA curve of neat PLA, neat PP and PP/PLA blend with nanosilica at different parts.

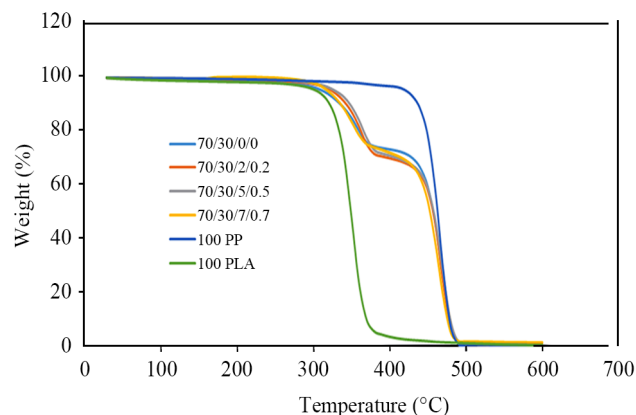


Figure 4. TGA curve of neat PLA, neat PP and PP/PLA blend with compatibilizer and nanosilica at different parts.

in the neat blend, there was a significant shift toward PLA in the blend, and the thermal stability of the blend was further improved by adding 2, 5, and 7 parts of the compatibilizer, respectively.

Thermal degradation of the PP/PLA pure blend, as well as other samples that contained 0.2, 0.5 and 0.7 parts of nanosilica, was shown in Figure 3. Downward shift was observed for 0.5 and 0.7 parts of nanosilica added samples in comparison with PP/PLA neat blend and neat PLA. Comparing neat PLA with the 0.2 parts nanosilica-based composition (Figure 3), the 0.2 parts composition exhibits better thermal stability than neat PLA. Additionally, its DTGA peak value is higher than that of neat PLA. But in the case of the 0.5 parts nanosilica composition, even though it has a higher DTGA peak value than neat PLA, there is a higher initial weight loss in the range of 300°C for the 0.5 parts composition leads for lower thermal stability compared to neat PLA. The DTGA peak provides information about the temperature at which maximum weight loss occurs per degree Celsius in that specific composition. The weight loss per degree Celsius at the DTGA peak is different for samples with different compositions; only the weight loss for that particular composition is higher at its DTGA peak.

In the initial weight loss in the range of 300°C region, these two individual materials do not reach the maximum weight loss per degree Celsius. However, there is more weight loss in the 0.5 parts compositions. After crossing 350 °C, neat PLA reaches maximum weight loss at 351.57 °C and 0.5 parts composition reaches maximum weight loss at 362.24°C. So, it is possible for a material like 0.5 parts nanosilica composition to have a lower thermal stability but with a higher DTGA peak value than another material like neat PLA with a lower DTGA peak value.

Table 3. Thermal degradation kinetic data (Composition: PP/PLA/PP-g-MA/Nanosilica).

Blends	E_a (kJ/mol)	R^2	A (Sec ⁻¹)	T_p (°C)	K (Sec ⁻¹)	ΔH (kJ/mol)	ΔS (J/mol)	ΔG (kJ/mol)
100 PLA	65.96	0.978	2.56E+05	351.57	0.7812	60.77	-17.748	71.85
70/30/0/0	90.22	0.997	7.84E+05	359.1	0.0775	84.97	-16.641	95.49
70/30/2/0	110.79	0.996	1.29E+08	364.12	0.0396	111.49	-11.546	108.85
70/30/5/0	120.12	0.992	7.49E+06	361.61	0.0346	96.84	-14.387	125.97
70/30/7/0	118.20	0.999	2.76E+08	366.44	0.0428	115.30	-10.788	122.20
70/30/0/0.2	90.82	0.999	1.60E+04	359.99	0.0777	64.56	-20.537	77.56
70/30/0/0.5	76.27	0.999	2.52E+06	362.24	0.0831	90.99	-15.476	75.82
70/30/0/0.7	63.16	0.998	5.55E+03	335.88	0.0852	58.10	-21.554	71.23
70/30/2/0.2	113.40	0.999	7.32E+07	363.5	0.0363	108.11	-12.110	115.82
70/30/5/0.5	121.82	0.997	1.09E+09	364.75	0.0342	122.52	-9.411	128.52
70/30/7/0.7	84.36	0.985	2.52E+05	353.45	0.0634	79.15	-17.767	90.29
100 PP	156.70	0.975	6.03E+09	463.92	0.0473	150.57	-7.844	156.35

[R^2 is a measure of the goodness of fit of a model. An R^2 of 1 indicates that the regression predictions perfectly fit the data.]

Inorganic nanoparticles like nanosilica are typically more thermally stable than PLA. Silica nanoparticles, for instance, can withstand high temperatures without undergoing significant degradation. Because of that, the 0.2 parts nanosilica based composition has better thermal stability than neat PLA. In this study, hydrophilic nanosilica was used as a nanoparticle to modify the blend material's properties. When

hydrophilic nanosilica content increased from 0.2 parts to 0.5 and 0.7 parts, especially during the temperature of melt blend process, the hydroxyl groups on the surface of nanosilica could increase the hydrolysis of ester groups in PLA. The most possible reason for the reduction in the thermal stability of PLA-based nanocomposites with 0.5 and 0.7 parts is this hydrolysis reaction.

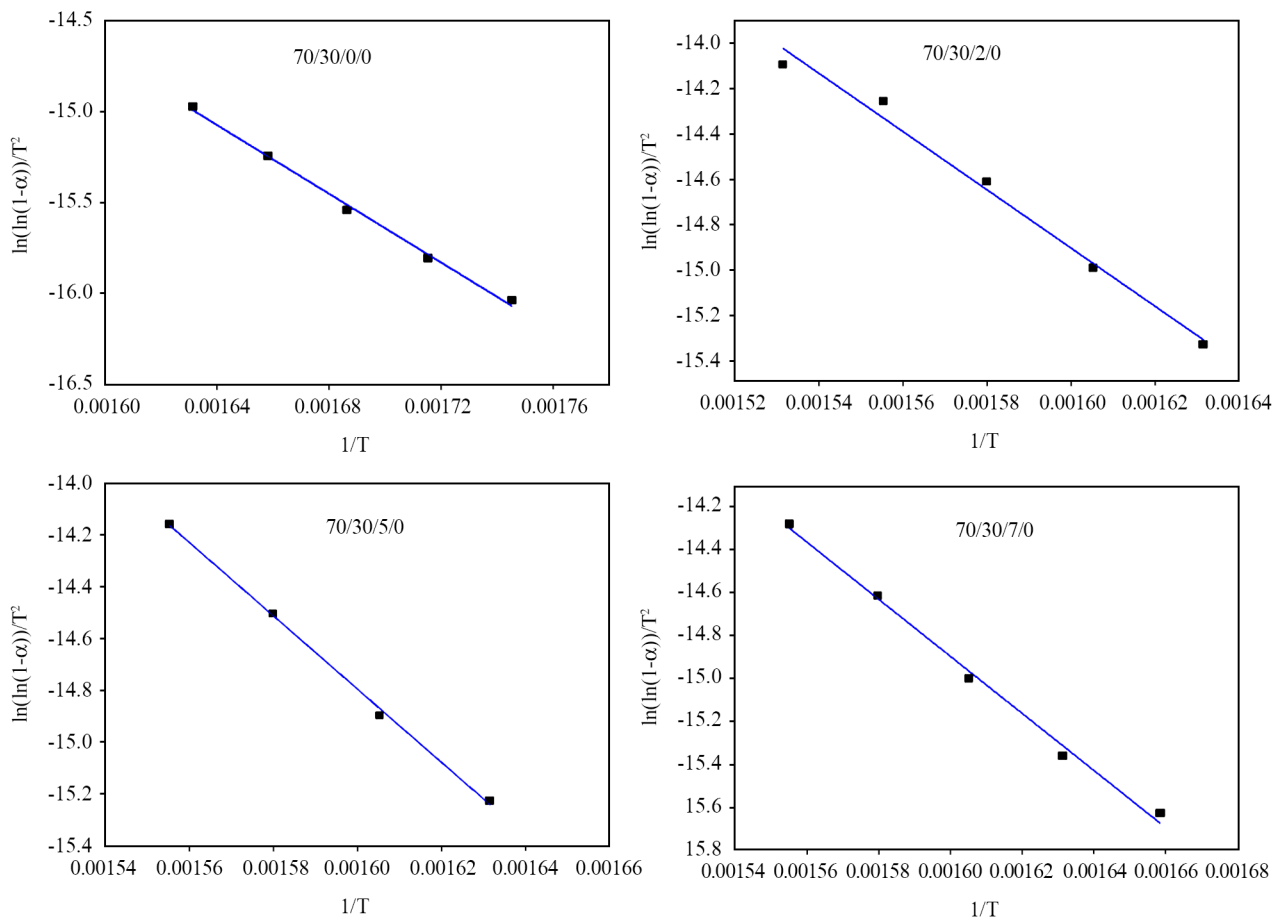
**Figure 5 (a).** Coats Redfern graph analysis for 2, 3 and 7 parts of compatibilizer.

Figure 4 shows the thermal degradation curve of a neat PP/PLA blend and other samples with nanosilica and compatibilizer added in various parts. Thermal stability was increased in polymer blends with PP-g-MA 2 parts, nanosilica 0.2 parts, and PP-g-MA 5 parts, nanosilica 0.5 parts. It indicates that the compatibilizer contributes to the increase in thermal stability of polymer blends [27-31]. A downward shift was observed in the case of PP-g-MA 7 parts with

nanosilica 0.7 parts. This may be due to reaching the critical level of nanofiller and compatibilizer, which leads to a dispersion problem.

As mentioned in "*Thermogravimetric analysis*", activation energy for thermal degradation of each composition and other parameters were calculated and shown in Table 3. The activation energies of neat PLA, neat PP and neat PP/PLA blend (70/30)

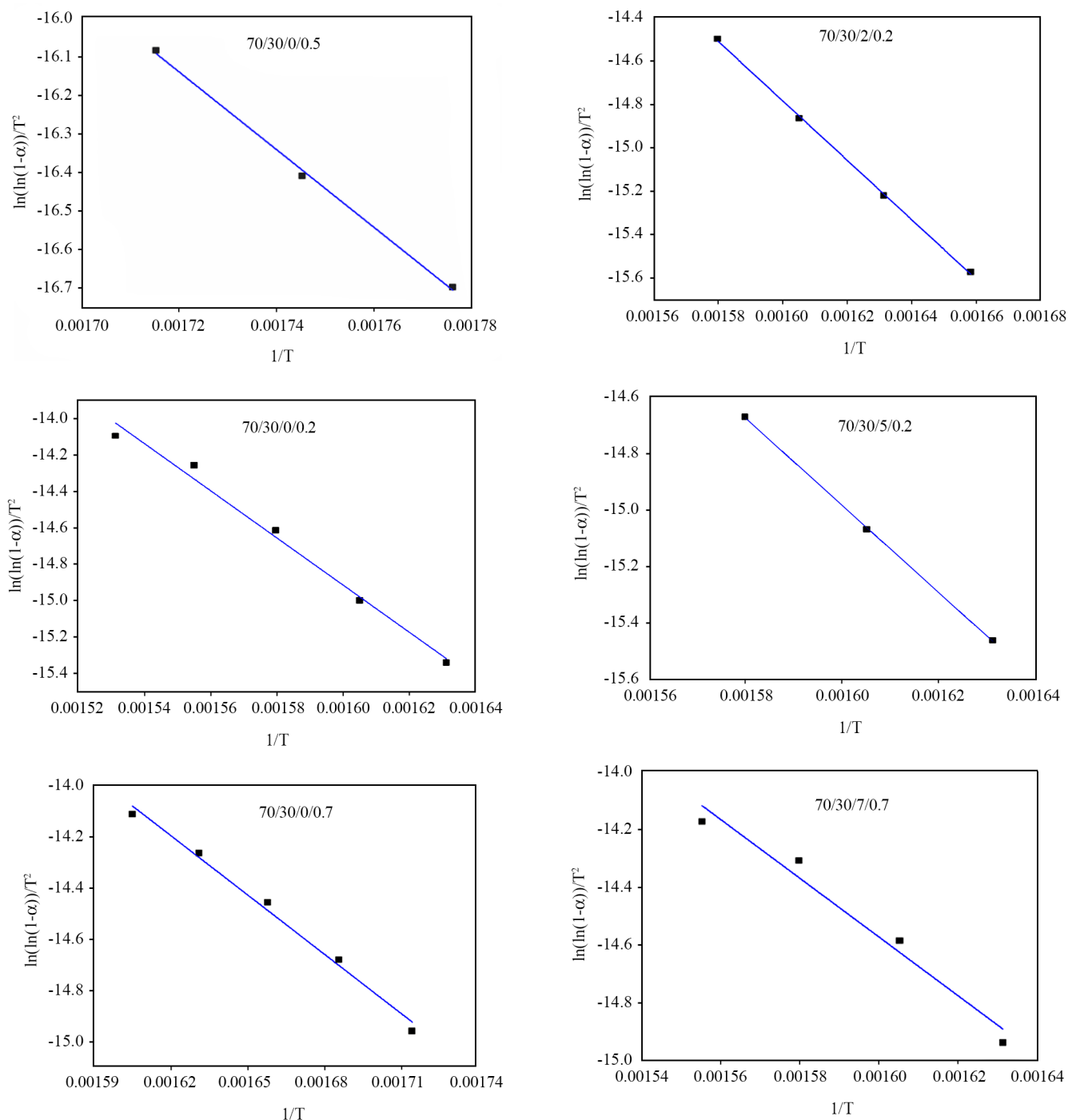


Figure 5 (b). Coats Redfern graph analysis for 0.2,0.5 and 0.7 parts of nanosilica.

Figure 5 (c). Coats Redfern graph analysis for (2,0.2), (5,0.5) and (7,0.7) parts of compatibilizer and silica.

were 65.96, 156.70 and 90.22 kJ/mol, respectively, based on the TGA graph (Figure 5). When 2, 5 and 7 parts compatibilizer were added to the neat blend, the activation energy increases from 90.22 to 110.79, 120.12 and 118.20 kJ/mol, respectively. Studies conducted on nanosilica based compositions have shown that activation energy for nanosilica based compositions is lower compared to the neat blend value. Polymer blends containing PP-g-MA 5 parts and PP-g-MA 5 parts with nanosilica 0.5 parts have the highest activation energy, indicating the highest thermal stability.

The high-rate constant value (K) of PLA indicates

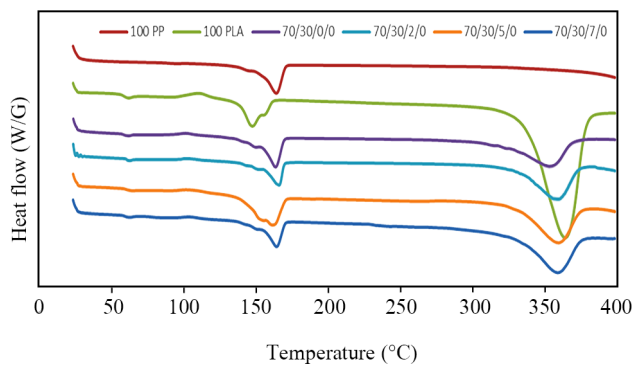


Figure 6. DSC analysis for different parts of compatibilizer.

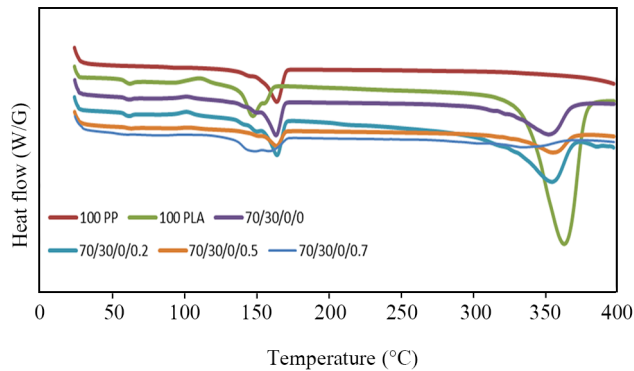


Figure 7. DSC analysis for different parts of nanosilica.

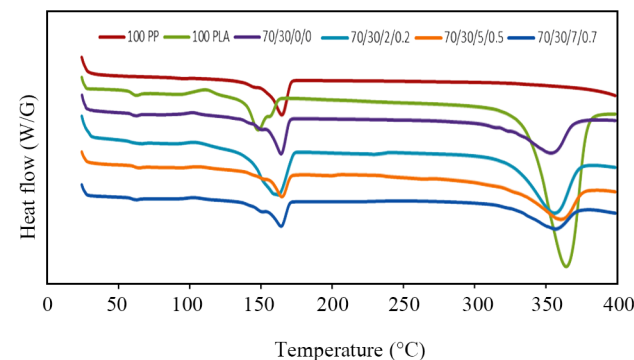


Figure 8. DSC analysis for different parts of compatibilizer and nanosilica.

that it degrades rapidly during thermal treatment. As compared with neat PLA, PLA degradation has been significantly reduced when blended with PP, as the rate constant K has decreased. A positive value for ΔH indicates that the decomposition reaction is endothermic, while a positive value for ΔG indicates that it is a non-spontaneous reaction.

Differential scanning calorimetry (DSC)

DSC analysis (Figure 6) revealed that the T_g , T_m , and crystallinity % of neat PLA were 59.8°C, 147.6°C, and 49.75, respectively. Figures 6, 7 and 8 show merged DSC graphs of compatibilizers with various parts, nanosilica with various parts, and compatibilizers and nano silica with various parts, respectively. In the DSC analysis of PP material, T_g was not detected, but T_m and crystallinity were found to be 166.8 °C and 28.69 %, respectively. A neat blend of PP/PLA (70/30) showed T_g and crystallinity % to be 58.9°C and 30.10, respectively. For neat PLA, cold crystallization was observed at 110.9°C, but in the blend, it shifted to in the range of 102°C. In the case of neat PLA, the cold crystallization enthalpy was 9.18 J/g and in case of the pure blend, it was 2.85 J/g, and in the case of compatibilizer-based blends, it was reduced to in the range of 1.4 J/g. T_g , T_m and crystallinity % of all samples were calculated and are shown in Table 4. This study shows that T_g of PLA tends to increase marginally for blends due to partial interaction in the blends, reducing chain mobility, especially in compatibilizer-based blends [32,33]. A marginal decrease in the T_m of the PP portion was observed in the PP/PLA blend, as well as in compositions with added nanosilica and compatibilizer. A small decrease in lamellae thickness and spherulite size in the compositions with compatibilizer and nanosilica is a possible reason for the decrease in the T_m value [12]. T_m values of crystalline polymers can be related to the size and perfection of crystal units.

Except for 70/30/0/0.7 composition, all blends composition has crystallinity % above neat PP. The presence of compatibilizer and nanosilica in the composition, increases the nucleation rate and crystallization rate, leading to a high crystallinity percentage [34].

Fourier Transform Infrared Spectroscopy (FTIR)

Figure 9 shows the FTIR spectra of neat PLA, neat PP, and other compositions. In PLA, stretching wavenumber were found at 1746, 2984, 2964, and 1087 cm^{-1} for C=O, C-H asymmetric, C-H symmetric,

Table 4. T_g , T_m and crystallinity % from DSC analysis.

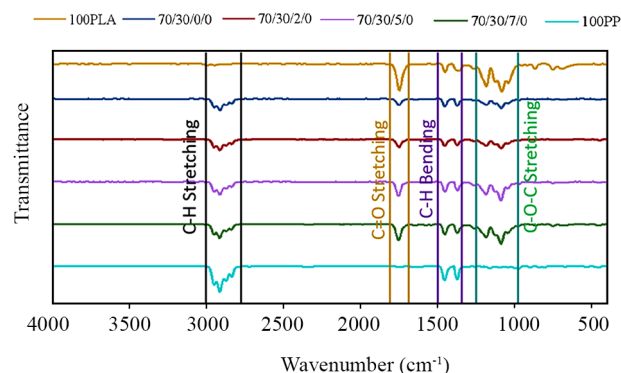
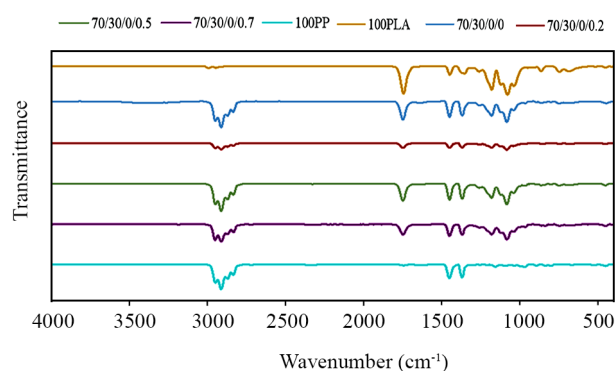
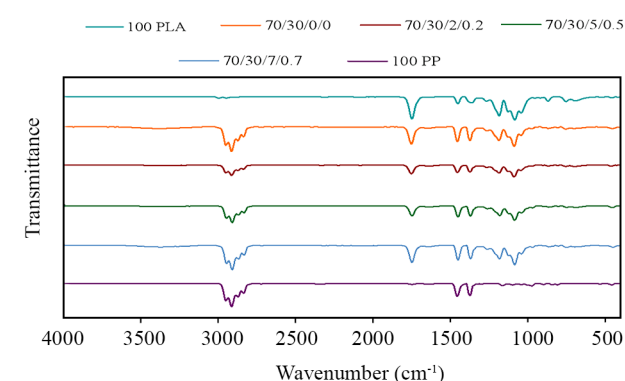
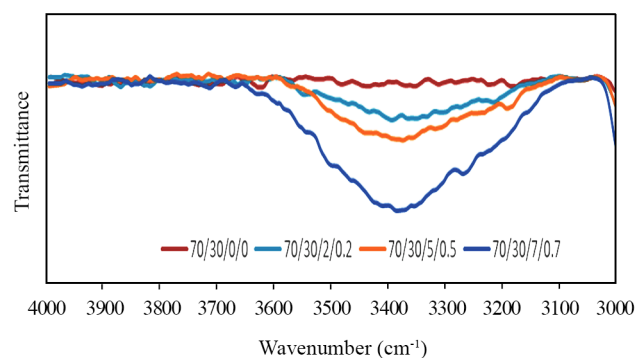
Sample composition	T_g (°C)	Melting point (PLA) (°C)	Melting point (PP) (°C)	Crystallinity %
70/30/0/0	58.9	149.9	163.6	30.10
70/30/2/0	61.2	152.7	166.3	34.48
70/30/5/0	62.1	153.8	161.9	40.90
70/30/7/0	61.1	151.3	165.2	33.87
70/30/0/0.2	60.0	149.9	164.9	31.39
70/30/0/0.5	60.8	151.7	164.7	32.35
70/30/0/0.7	55.4	145.6	163.1	26.73
70/30/2/0.2	61.5	153.7	162.5	41.05
70/30/5/0.5	61.7	152.0	164.9	36.33
70/30/7/0.7	59.9	150.3	164.3	32.44
100% PP	-	-	166.8	28.69
100% PLA	59.8	147.6	-	49.75

and C–O, respectively. Both C–H (methylene group) and C–H (methyl group) bend were identified at 1458 and 1374 cm^{-1} respectively. PP showed its main peak at 2900 range cm^{-1} , 1464 cm^{-1} and 1388 cm^{-1} for C–H asymmetric and symmetric stretching, and C–H bending (methylene group) and bending (methyl group), respectively [1,5,12].

A FTIR spectrum (Figure 9(a) and 9(b)) of neat PP/PLA blend, blend with only compatibilizer (2,5 and 7 parts) and blend with only nanosilica (0.2,0.5 and 0.7 parts) shows all peak positions corresponding to PP and PLA. But in the case of both compatibilizer and nanosilica added blend composition shows (Figure 9(c) and 9(d)) an extra peak in the range of 3100–3500 cm^{-1} . This peak intensity increases from 70/30/0/0 to 70/30/7/0.7 composition. This peak intensity increases directly with when both the compatibilizer parts and nanosilica parts are increased. Peak presence in this region indicates that hydrogen bonding formation is possible between compatibilizer and nanosilica.

Field emission scanning electron microscope (FE SEM)

A scanning electron microscope image was taken from a fractured surface of the specimen used for the tensile test. PP is in continuous phase, and PLA is in discontinuous phase. Figure 10 shows a blending of two partially miscible materials that resulted in discontinuous PLA holes in a continuous PP matrix. During the tensile test failure, PLA was pulled out, as indicated by the holes. Hole sizes decreased in this blend when compatibilizers were added. For 2 and 5 parts of the compatibilizer, the hole size decreased, but for 7 parts it increased again (Figure 10). For 7 parts composition, this may be caused by agglomeration and poor dispersion of PP-g-MA. In another study

**Figure 9(a).** FTIR analysis for various parts of compatibilizer.**Figure 9(b).** FTIR analysis for various parts of nanosilica.**Figure 9(c).** FTIR analysis for various parts of compatibilizer and nanosilica.**Figure 9(d).** FTIR analysis for various parts of compatibilizer and nanosilica (wave number from 3000 to 4000 cm^{-1}).

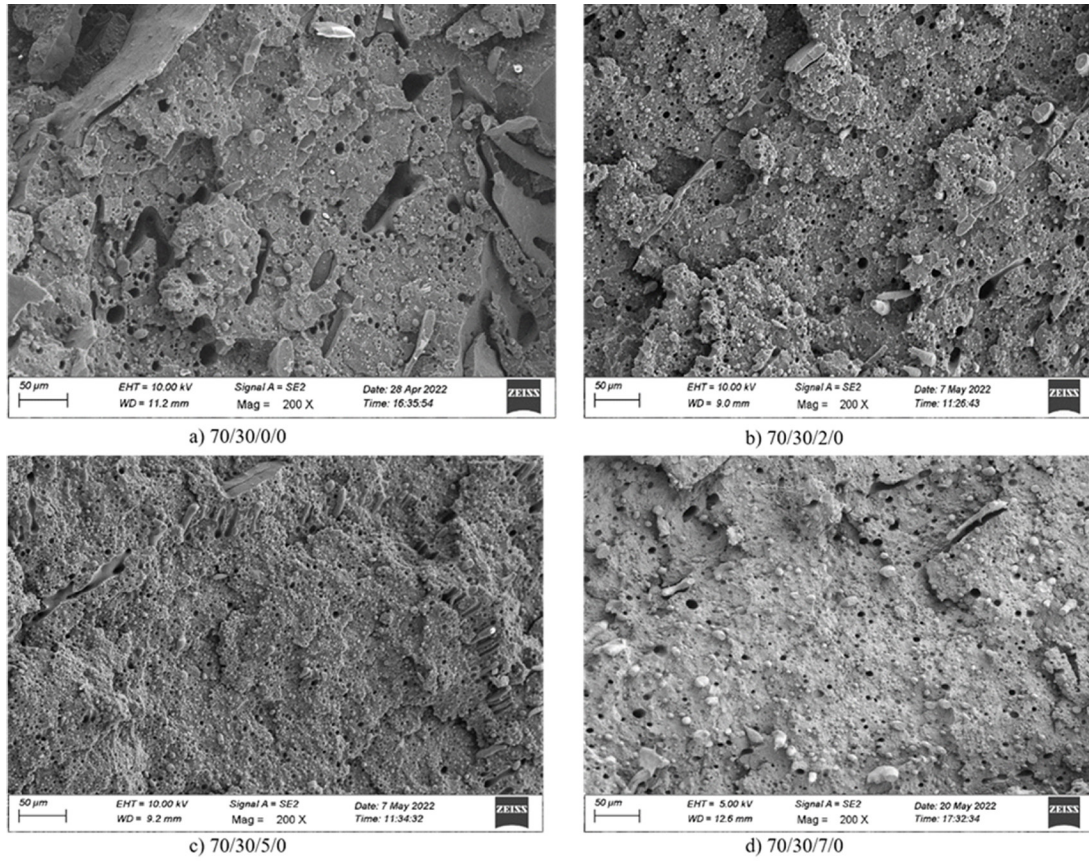


Figure 10. SEM images of PP/PLA blend with various parts of compatibilizer.

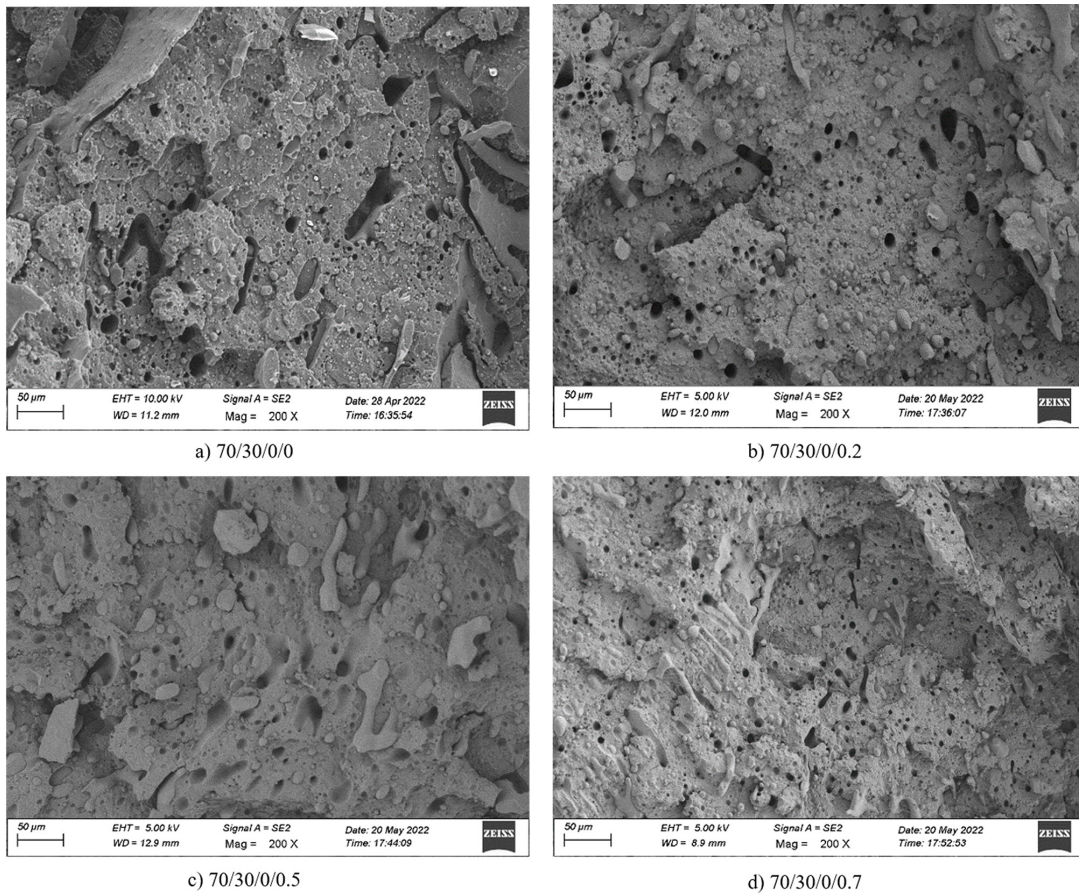


Figure 11. SEM images of PP/PLA blend with various parts of nanosilica.

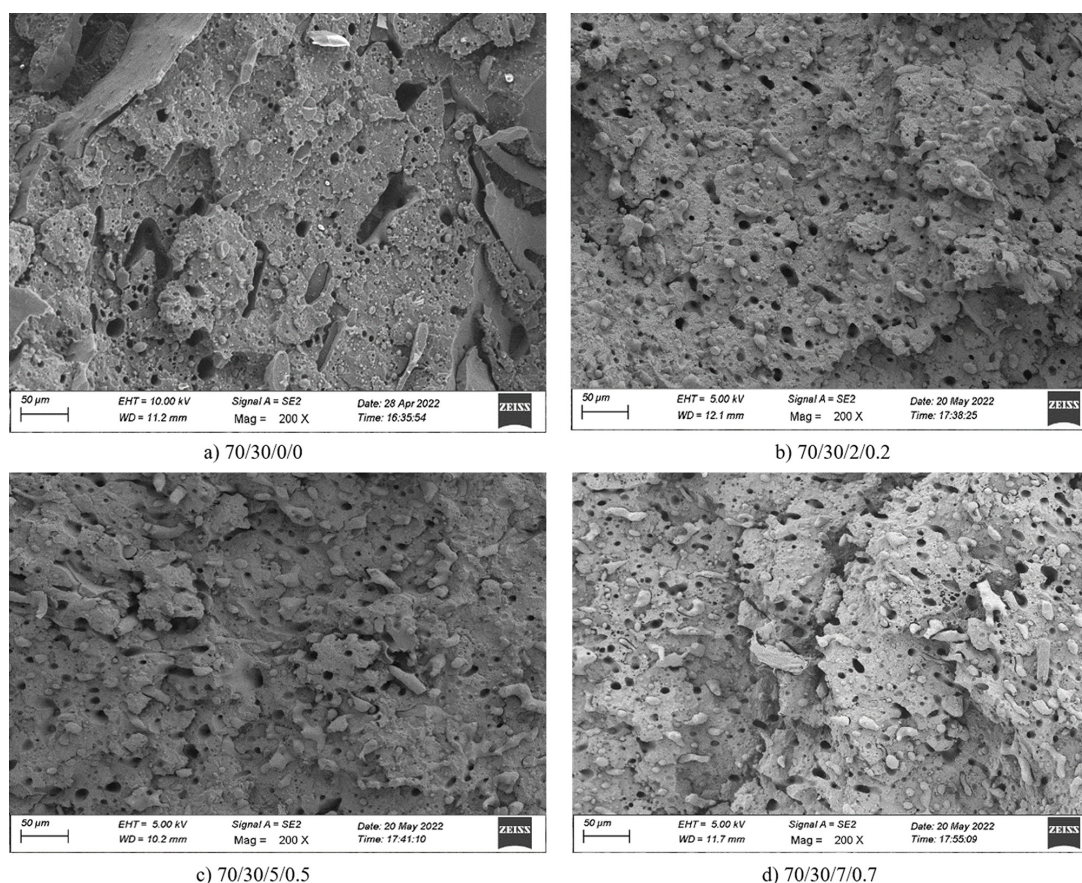


Figure 12. SEM images of PP/PLA blend with various parts of compatibilizer and nanosilica.

(Figure 11), nanosilica in amounts of 0.2, 0.5, and 0.7 parts were added to this PP/PLA blend and the results were analyzed with SEM. However, in this case, there was no significant reduction in hole size. In blend material containing nanosilica and compatibilizer (Figure 12), a reduction in hole size was observed in 70/30/5/0.5 and 70/30/7/0.7 composition. A reduction in hole size in the SEM image indicates a reduction in dispersed PLA domain size and an improvement in compatibility. The studies indicated that PP/PLA compatibility had indeed improved with the compatibilizer based composition [35,36].

The samples exhibit matrix-droplet morphology where PLA and PP act as the dispersed and matrix phases, respectively. These micrographs demonstrate the uniform distribution of PLA dispersed droplets within the PP matrix. When comparing the PLA droplet sizes in the SEM micrographs of the neat PP/PLA (70/30) blend, it becomes evident that the average size of the PLA domains starts to decrease after the addition of 3 and 5 parts of compatibilizer. The decrease in the size of PLA domains increases the contact area between them, leading to improved interfacial adhesion, and minimizes stress concentration. This

improved interfacial adhesion contributes to better tensile strength, modulus, and elongation in the blend.

In this scenario, the compatibilizer serves as a conduit bridging the distinct PP and PLA phases, thereby promoting a better dispersion of PLA within the PP phase. The nonpolar segment of the PP-g-MA compatibilizer engages with the PP components in the blend, while the maleic anhydride moiety of the compatibilizer has an affinity with the -OH end group and polyester group of PLA.

CONCLUSION

A PP-based blend was prepared using PLA and PP-g-MA/nanosilica to enhance the tensile strength and modulus of PP and to support sustainability initiatives by incorporating biodegradable and renewable components (PLA) into this blend. The blend was then characterized using various methods. It has been found that PP-g-MA was effective as a compatibilizer in improving blend's tensile strength, modulus, and elongation. The 5 parts compatibilizer has shown improved tensile properties compared to 2 and 7 parts.

The compatibility between PP and PLA was improved upon adding compatibilizer, since the nonpolar segment of compatibilizer interacted with PP and MA moiety interacted with ester groups and chain end hydroxyl groups of PLA. The more hydrophilic nature of nanosilica, unable to interact with the blend system, is making nanosilica less effective in improving blend's tensile strength. However, due to its reinforcement effect, it does improve the modulus. According to the DSC studies, the compositions based on 5 parts of compatibilizer exhibit high T_g and crystallinity percentage in the blend, indicating improved compatibility between PP and PLA in this composition.

A TGA study showed that adding a compatibilizer to PP based blend improved its thermal stability. In the case of nanosilica based blend, thermal stability is eroded, however when added with compatibilizer, blend's thermal stability improves. Based on TGA results, activation energy, rate constant, ΔH , and ΔG were calculated, suggesting the compatibilizer-based composition is more thermally stable. It was found that the FTIR spectra of PP/PLA/PP-g-MA/nanosilica composition revealed a broad peak in the range of 3000-3500 cm^{-1} which implies the presence of the intermolecular hydrogen bond between OH of nanosilica and maleic anhydride reactive group. Intensity of the band increased from 70/30/2/0.2 to 70/30/7/0.7 as the amount of compatibilizer and nanosilica increased.

ACKNOWLEDGEMENTS

The authors gratefully acknowledge the support of the Center of Excellence for Advanced Materials and Green Technologies (CoE-AMGT), Amrita Vishwa Vidyapeetham (Amrita University), Coimbatore for providing facilities for material characterization and testing.

CONFLICTS OF INTEREST

The authors declare that they have no conflicts of interest.

REFERENCES

1. Rajan KP, Gopanna A, Abdelghani EA, Thomas

- SP (2021) Halloysite nanotubes (HNT) as reinforcement for compatibilized blends of polypropylene (PP) and polylactic acid (PLA). *J Polym Res* 28: 374
2. Hamad K, Kaseem M, Deri F (2011) Rheological and mechanical characterization of poly(lactic acid)/polypropylene polymer blends. *J Polym Res* 18: 1799-1806
3. Aghjeh MR, Asadi V, Mehdijabbar P, Khonakdar HA, Jafari SH (2016) Application of linear rheology in determination of nanoclay localization in PLA/EVA/Clay nanocomposites: Correlation with microstructure and thermal properties. *Compos B Eng* 86: 273-284
4. Shah TV, Vasava DV (2019) A glimpse of biodegradable polymers and their biomedical applications. *E-Polym* 19: 385-410
5. Arrieta MP, Fortunati E, Dominici F, López J, Kenny JM (2015) Bionanocomposite films based on plasticized PLA-PHB/cellulose nanocrystal blends. *Carbohydr Polym* 121: 265-275
6. Deghiche A, Haddaoui N, Zerriouh A, Fenni SE, Cavallo D, Erto A, Benguerba Y (2021) Effect of the stearic acid-modified TiO₂ on PLA nanocomposites: Morphological and thermal properties at the microscopic scale. *J Environ Chem Eng* 9: 106541
7. Zhao X, Hu H, Wang X, Yu X, Zhou W, Peng S (2020) Super tough poly(lactic acid) blends: A comprehensive review. *RSC Adv* 10: 13316-13368
8. Castro-Aguirre E, Iñiguez-Franco F, Samsudin H, Fang X, Auras R (2016) Poly(lactic acid) –mass production, processing, industrial applications, and end of life. *Adv Drug Deliv Rev* 107: 333-366
9. Jem KJ, Tan B (2020) The development and challenges of poly (lactic acid) and poly (glycolic acid). *Adv Ind Eng Polym Res* 3: 60-70
10. Guopeng S, Mengfan J, Jing Z, Ke W, Qin Z, Qiang F (2018) A comparison study of high shear force and compatibilizer on the phase morphologies and properties of polypropylene/poly lactide (PP/PLA) blends. *Polymer* 154: 119-127
11. Xu Y, Loi J, Delgado P, Topolkarav V, McEneaney RJ, Macosko CW, Hillmyer MA (2015) Reactive compatibilization of polylactide/polypropylene blends. *Ind Eng Chem Res* 54: 6108-6114
12. Choudhary P, Mohanty S, Nayak SK,

- Unnikrishnan L, (2011) Poly(L-lactide)/ Polypropylene Blends: Evaluation of mechanical, thermal, and morphological characteristics. *J Appl Polym Sci* 121: 3223-3237
13. Rajan KP, Thomas SP, Gopanna A, Al-Ghamdi A, Chavali M (2018) Rheology, mechanical properties and thermal degradation kinetics of polypropylene (PP) and polylactic acid (PLA) blends. *Mater Res Express* 5: 085304
 14. Yoo TW, Yoon HG, Choi SJ, Kim MS, Kim YH, Kim WN (2010) Effects of compatibilizers on the mechanical properties and interfacial tension of polypropylene and poly(lactic acid) blends. *Macromol Res* 18: 583-588
 15. Ebadi-Dehaghani H, Khonakdar HA, Barikani M, Jafari SH, Wagenknecht U, Heinrich G (2016) An investigation on compatibilization threshold in the interface of polypropylene/polylactic acid blends using rheological studies. *Vinyl Addit Technol* 22: 19-28
 16. Li X, Yang Q, Zhang K, Pan L, Feng Y, Jia Y, Xu N (2022) Property improvement and compatibilization mechanism of biodegradable polylactic acid/maleic anhydride-based/polypropylene spunbonded nonwoven slices. *J Clean Prod* 375: 134097
 17. Bhasney SM, Kumar A, Katiyar V (2020) Microcrystalline cellulose, polylactic acid and polypropylene biocomposites and its morphological, mechanical, thermal and rheological properties. *Compos B Eng* 184: 107717
 18. Bai Z, Dou Q (2018) Rheology, morphology, crystallization behaviors, mechanical and thermal properties of poly(lactic acid)/polypropylene/maleic anhydride-grafted polypropylene blends. *J Polym Environ* (2018) 26: 959-969
 19. Mandal DK, Bhunia H, Bajpai PK, Chaudhari CV, Dubey KA, Varshney L, Kumar A (2021) Preparation and characterization of polypropylene/ polylactide blends and nanocomposites and their biodegradation study. *J Thermoplast Compos Mater* 34 (2021) 725-744
 20. Dastakeer S, Saminathan P, Venkatesan S, Sudha PG, Kannan M (2019) Studies on thermal degradation kinetics and dielectric properties of polyether imide foam/nanosilica-based nanocomposites. *Plast Rubber compos* 48: 356-363
 21. Anbupalani MS, Venkatachalam CD, Rathanasamy R (2020) Influence of coupling agent on altering the reinforcing efficiency of natural fibre-incorporated polymers – A review. *J Reinf Plast Compos* 39: 520-524
 22. Zhang T, Chen X, Guo Z, Xiu H, Bai H, Zhang Q, Fu Q (2021) Controlling the selective distribution of hydrophilic silica nanoparticles in polylactide/ethylene-co-vinyl-acetate blends via tailoring the OH surface concentration of silica. *Compos Commun* 25: 100737
 23. Luiz CCJ, Janaïne MO, Rosineide ML, Beltrami LR, Zattera AJ, AnflorCT M, Doca TCR, Luz SM (2022) Tensile behavior analysis combined with digital image correlation and mechanical and thermal properties of microfibrillated cellulose fiber/ polylactic acid composites. *Polym Test* 113: 107665
 24. Eichers M, Bajwa D, Shojaeiarani J, Bajwa S (2022) Biobased plasticizer and cellulose nanocrystals improve mechanical properties of polylactic acid composites. *Ind Crops Prod* 183: 114981
 25. Eastwood E, Viswanathan S, O'Brien CP, Kumar D, Dadmun MD (2005) Methods to improve the properties of polymer mixtures: optimizing intermolecular interactions and compatibilization. *Polymer* 46: 3957-3970
 26. Zhou Y, Fan M, Chen L (2016) Interface and bonding mechanisms of plant fibre composites: An overview. *Compos B Eng* 101: 31-45
 27. Carrasco F, Pérez-Maqueda LA, Santana OO, MasPOCH MLI (2014) Enhanced general analytical equation for the kinetics of the thermal degradation of poly(lactic acid)/ montmorillonite nanocomposites driven by random scission. *Polym Degrad Stab* 101: 52-59
 28. Zou D, Zheng X, Ye Y, Yan D, Xu H, Si S, Li X (2022) Effect of different amounts of bamboo charcoal on properties of biodegradable bamboo charcoal/polylactic acid composites. *Int J Biol Macromol* 216: 456-464
 29. Loyo C, Moreno-Serna V, Fuentes J, Amigo N, Sepúlveda FA, Ortiz JA, Rivas LM, Ulloa MT, Benavente R, Zapata PA (2022) PLA/ CaO nanocomposites with antimicrobial and photodegradation properties. *Polym Degrad Stab* 197: 109865
 30. Lai SM, Wu SH, Lin GG, Don TM (2014) Unusual mechanical properties of melt-blended poly(lactic acid) (PLA)/clay nanocomposites.

- Eur Polym J 52: 193-206
31. Vinodhini J, Pitchan MK, Bhowmik S, Barandun GA, Jousset P (2020) Effect of different filler reinforcement on poly-ether-ether-ketone based nanocomposites for bearing applications. *J Compos Mater* 54: 4709-4722
 32. Zhou YM, Fu SY, Zheng LM, Zhan HY (2012) Effect of nanocellulose isolation techniques on the formation of reinforced poly(vinyl alcohol) nanocomposite films. *Express Polym Lett* 6: 794-804
 33. Scaffaro R, Sutura F, Mistretta M C, Botta L, La Mantia F P (2017) Structure-properties relationships in melt reprocessed PLA/hydroxycitric acid nanocomposites. *Express Polym Lett* 11: 555-564
 34. Coba-Daza S, Carmeli E, Otaegi I, Aranburu N, Guerrica-Echevarria G, Kahlen S, Cavallo D, Tranchida D, Müller AJ (2022) Effect of compatibilizer addition on the surface nucleation of dispersed polyethylene droplets in a self-nucleated polypropylene matrix. *Polymer* 263: 12551
 35. Sarath Kumar P, Jayanarayanan K, Balachandran M (2022) Performance comparison of carbon fiber reinforced polyaryletherketone and epoxy composites: Mechanical properties, failure modes, cryo-thermal behavior, and finite element analysis. *J Appl Polym Sci* 139: 52494
 36. Xiu H, Huang C, Bai H, Jiang J, Chen F, Deng H, Wang K, Zhang Q, Fu Q (2014) Improving impact toughness of polylactide/poly(ether)urethane blends via designing the phase morphology assisted by hydrophilic silica nanoparticles. *Polymer* 55: 1593-1600